

## Article

# Characterization and Antimicrobial Activity of a Halophyte from the Asturian Coast (Spain): *Limonium binervosum* (G.E.Sm.) C.E.Salmon

Eva Sánchez-Hernández <sup>1</sup>, Laura Buzón-Durán <sup>1</sup>, Natalia Langa-Lomba <sup>2</sup>, José Casanova-Gascón <sup>2</sup>, Belén Lorenzo-Vidal <sup>3</sup>, Jesús Martín-Gil <sup>1</sup> and Pablo Martín-Ramos <sup>2,\*</sup>

- <sup>1</sup> Agriculture and Forestry Engineering Department, ETSIIAA, Universidad de Valladolid, Avenida de Madrid 44, 34004 Palencia, Spain; eva.sanchez.hernandez@uva.es (E.S.-H.); laura.buzon@uva.es (L.B.-D.); mgil@iaf.uva.es (J.M.-G.)
- <sup>2</sup> Instituto Universitario de Investigación en Ciencias Ambientales de Aragón (IUCA), EPS, Universidad de Zaragoza, Carretera de Cuarte, s/n, 22071 Huesca, Spain; natalialangalomba@gmail.com (N.L.-L.); jcasan@unizar.es (J.C.-G.)
- <sup>3</sup> Servicio de Microbiología, Hospital Universitario Río Hortega, Calle Dulzaina 2, 47012 Valladolid, Spain; blorenzov@saludcastillayleon.es
- \* Correspondence: pmr@unizar.es



**Citation:** Sánchez-Hernández, E.; Buzón-Durán, L.; Langa-Lomba, N.; Casanova-Gascón, J.; Lorenzo-Vidal, B.; Martín-Gil, J.; Martín-Ramos, P. Characterization and Antimicrobial Activity of a Halophyte from the Asturian Coast (Spain): *Limonium binervosum* (G.E.Sm.) C.E.Salmon. *Plants* **2021**, *10*, 1852. <https://doi.org/10.3390/plants10091852>

Academic Editors: Adam Stebel and Maria Iorizzi

Received: 7 August 2021

Accepted: 4 September 2021

Published: 7 September 2021

**Publisher's Note:** MDPI stays neutral with regard to jurisdictional claims in published maps and institutional affiliations.



**Copyright:** © 2021 by the authors. Licensee MDPI, Basel, Switzerland. This article is an open access article distributed under the terms and conditions of the Creative Commons Attribution (CC BY) license (<https://creativecommons.org/licenses/by/4.0/>).

**Abstract:** The work presented herein deals with the characterization and valorization of a halophyte from the cliffs of the Asturian coast: *Limonium binervosum* (G.E.Sm.) C.E.Salmon (rock sea-lavender). Its biomass and hydromethanolic extracts were studied by elemental and thermal analysis, infrared spectroscopy and gas chromatography–mass spectroscopy. Tetradecanoic acid/esters and 1,2-tetradecanediol were identified in its flower extract, while the leaf extract was rich in linolenic and linoleic acids and their esters, hexadecanoic acid and its esters, and phytol. Both flower and leaf hydromethanolic extracts contained eicosane, sitosterol and tocopherols in significant amounts. With a view to its valorization, the antimicrobial activity of these extracts was investigated against three apple tree and grapevine phytopathogens. Both the hydroalcoholic extracts and their main constituents, alone or in combination with chitosan oligomers (COS), were tested in vitro. A remarkable antibacterial activity was observed for the conjugated complexes of the flower extract with COS, both against *Xylophilus ampelinus* (MIC = 250 µg·mL<sup>-1</sup>) and *Erwinia amylovora* (MIC = 500 µg·mL<sup>-1</sup>), and complete inhibition of the mycelial growth of *Diplodia seriata* was found at concentrations <1000 µg·mL<sup>-1</sup>. In view of these results, this extremophile plant can be put forward as a promising source of bioactive metabolites.

**Keywords:** antibacterial; antifungal; *Diplodia seriata*; *Erwinia amylovora*; rock sea lavender; *Xylophilus ampelinus*

## 1. Introduction

*Limonium* is one of the most important species-rich genera in the *Plumbaginaceae* family. This widespread genus of halophytes and taxa includes sexual diploids of the *L. ovalifolium* (Poir.) Kuntze complex, the triploid *L. algarvense* Erben and the agamosperous tetraploids of the *L. binervosum* (G.E.Sm.) C.E.Salmon complex [1]. The *L. binervosum* aggregate is a species group that has not been assigned to any of the subsections of *L. sect. Limonium* [2] and was first reported in 1922 by Salmon [3].

The habitat of *L. binervosum* includes coastal cliffs, pebble beach margins, steppes, meadows and lagoons. It grows on the Atlantic coasts of Europe, from the south-west United Kingdom and north-west France to northern Spain, with a number of geographically restricted segregate taxa (Figure 1a).



activity of its extracts—alone and in combination with chitosan oligomers—against aforementioned phytopathogens.

## 2. Results

### 2.1. Elemental Analysis and Calorific Values Calculation

The C, H, N and S percentages of *L. binervosum* components (wt% of dry material) were in the 40.5–44.7%, 6.4–6.5%, 1.2–2.6% and 0.2–0.9% range, respectively (Table 1).

**Table 1.** Elemental composition (wt%) of *L. binervosum* fractions.

Fraction	C	H	N	S	O	C/N Ratio
Flowers	44.7%	6.5%	1.3%	0.3%	47.2%	34.9
Leaves	40.5%	6.4%	2.6%	0.9%	49.6%	15.7

Higher heating values derived from elemental analysis data resulted in heating values for flowers and leaves of 18 and 16 kJ·g<sup>−1</sup>, respectively.

### 2.2. Thermal Analyses

The TG, DTG and DSC curves of flowers and leaves are shown in Figures S1 and S2, respectively. In the case of flowers, exothermal effects were detected at 329, 420 and 470 °C; the ash content (at 550 °C) was 5.6%. Concerning leaves, exothermal effects were registered at 320 and 470 °C, and the ash content (at 580 °C) reached 17%. For comparison purposes, the total ash content reported *L. stocksii* (Boiss.) Kuntze was 11.83% [18].

### 2.3. Vibrational Characterization

The main absorption bands in the FTIR spectra of the powdered dry samples of flowers and leaves are summarized in Table 2, together with their assignments. The bands at 2918, 2850, 1462 and 720 cm<sup>−1</sup> are due to aliphatic features and are present in straight-chain alkanes (compatible with the presence of tetracosane, pentacosane, heptacosane, etc., identified by GC–MS in the extracts, as discussed below) [19]. The band at 2158 cm<sup>−1</sup>, ascribed to C–N stretching, may arise from the presence of carbonitrogenated compounds (e.g., n-methyl-1-adamantaneacetamide; 2-(4-fluoro-phenyl)-4-(3-methyl-benzylidene)-4h-oxazol-5-one, 2-ethylacridine, etc.) [20]. The bands at ca. 1730 and ca. 1165 cm<sup>−1</sup>, related to carbonyl (C=O) stretching and C–C(=O)–O stretching, respectively, illustrate the main spectral features of esters (e.g., 2-hydroxy-tetradecanoic acid methyl ester; hexadecanoic acid methyl ester; 9,12-octadecadienoic acid methyl ester; 9,12,15-octadecatrienoic acid methyl ester, etc.) [19]. The band at ca. 1640 cm<sup>−1</sup>, resulting from C=O and C=C stretching vibrations and asymmetric N–H bending vibrations, can be due to flavonoids and lipids [21,22]. The bands at 1513 and 1417 cm<sup>−1</sup>, related to aromatic C=C stretching, are compatible with the presence of flavonoids and aromatic rings. The band at 1235 cm<sup>−1</sup> may be due to C–O group vibration in polyols, such as hydroxyflavonoids [23].

The FTIR spectrum of the lyophilized flower hydromethanolic extract (not included in Table 2) showed bands at 3362, 2917, 2849, 1733sh, 1636, 1462, 1340, 1228, 1067 and 957 cm<sup>−1</sup>, attributable to tetradecanoic (1727, 1448, 1310 cm<sup>−1</sup>) and eicosane (2914, 2847 and 1471 cm<sup>−1</sup>).

### 2.4. Hydromethanolic Extracts Characterization

#### 2.4.1. Phenolic Contents

The total phenolic content of the flower and leaf extracts were 162 ± 7 and 58 ± 2 mg GAE/g DW, respectively.

**Table 2.** Main bands in the FTIR spectra of *L. binervosum* flowers and leaves and their assignments. Peak positions are expressed in  $\text{cm}^{-1}$ .

Fraction		Assignment
Flowers	Leaves	
	3382	Bonded O–H stretching (cellulose)
2921	2918	–CH <sub>2</sub> asymmetric stretching of alkyls
2852	2850	–CH <sub>2</sub> symmetric stretching; CH <sub>2</sub> –(C6)– bending (cellulose)
2158		CN stretching
1731	1728	C=O stretching of alkyl ester
1653	1636	Amide I; C=C stretching; C=O stretching
1605	1617	Aromatic C=C skeletal stretching; COO <sup>−</sup> antisymmetric stretching (polygalacturonic, pectin ester)
1558		Amide II; COO <sup>−</sup> symmetric stretching; polynuclear aromatics
1515	1517	C=C stretching vibrations of aromatic structures
1457	1462	O–CH <sub>3</sub> stretching; C–H bending of CH <sub>2</sub> or CH <sub>3</sub>
1441	1417	CH <sub>2</sub> symmetric bending; aromatic C=C; COO symmetric stretching
1362	1372	C–H (cellulose)
1236	1236	Amide III; C–C–O asymmetric stretching acetylated glucomannan; C–O stretching of aryl ether; C–O and OH of COOH groups
1162	1168	C–O–C in bridge asymmetric; C–C in plane
1100	1104	C–O–C symmetric stretching
1017	1021	C–H bending (typical of carotenes); polygalacturonic acid (a variety of pectin in plant cuticles)
	874	$\beta$ -glycosidic linkages (glucose units of cellulose chains)
832	830	O–C=O in-plane deformation or a CH <sub>2</sub> rocking deformation
720		In-plane bending or rocking of the methylenes (–CH <sub>2</sub> –)
668		C–C out-of-plane bending

#### 2.4.2. Analysis of Hydromethanolic Extracts by GC–MS

The main constituents identified in the flower hydromethanolic extract (Tables 3 and S1, and Figure S3) were: tetradecanoic acid and methyl 2-hydroxy tetradecanoate (22%); eicosane (18%); 1,2-tetradecanediol (15%); sitosterol (9%); tocopherols/vitamin E (7%); and *n*-alkanes (heneicosane, tetracosane, pentacosane, heptacosane, etc., which add up to 6%). Among the minority constituents, it is necessary to highlight the presence of 2-ethyl-acridine (1.6%) as the only carbonitrogenated compound.

Concerning the main phytoconstituents identified in the leaf extract (Tables 4 and S2, and Figure S4), they were: octadecatrienoic acid (linolenic acid) and their esters (above 22%); sitosterol (19%); hexadecanoic acid and their esters (above 15%); octadecadienoic acid or linoleic acid (8%); vitamin E (8%) and other tocopherols (5%); trans-pinane (5%); eicosane (4%); and phytol (4%).

### 2.5. Antimicrobial Activity

#### 2.5.1. In Vitro Antibacterial Activity

The inhibition of flower and leaf extracts against *X. ampelinus* and *E. amylovora* were similar and comparable to that attained with COS (Table 5). Regarding the activities of the main active principles present in the extracts, differences were observed as a function of the pathogen: while tetradecanoic acid, linolenic acid and vitamin E showed similar activity against *X. ampelinus* (MIC = 500  $\mu\text{g}\cdot\text{mL}^{-1}$ ), tetradecanoic acid was the most effective against *E. amylovora* (MIC = 500  $\mu\text{g}\cdot\text{mL}^{-1}$ ), and linolenic acid and vitamin E were less effective (MIC = 750  $\mu\text{g}\cdot\text{mL}^{-1}$ ).  $\beta$ -sitosterol showed worse performance than the former three (MIC = 1000 and 1500  $\mu\text{g}\cdot\text{mL}^{-1}$  against *X. ampelinus* and *E. amylovora*, respectively), and eicosane was the least effective (MIC = 1000 and >1500  $\mu\text{g}\cdot\text{mL}^{-1}$  against *X. ampelinus* and *E. amylovora*, respectively).

**Table 3.** Main compounds identified in *L. binervosum* flower hydromethanolic extract by GC-MS.

Peak	R <sub>t</sub> (min)	Area (%)	Assignment	MW (Da)	Qual
2	11.842	0.92	geranyl acetate or 2,6-octadien-1-ol, 3,7-dimethyl-, acetate (stereoisomers)	196.3	90; 86
3	17.154	1.03	bicyclo[3.1.1]heptane, 2,6,6-trimethyl-, (1 $\alpha$ ,2 $\beta$ ,5 $\alpha$ ) (also named <i>trans</i> -pinane)	138.3	90
6	18.405	4.94	tetradecanoic acid	228.4	93
7	19.666	1.07	heneicosane; hexacosane	296.6; 366.7	98; 92
11	21.458	17.61	eicosane; hexadecane, 2,6,10,14-tetramethyl-; heptadecane	282.5; 282.5; 240.5	97; 97; 96
13	23.060	3.36	heneicosane; pentacosane	296.6; 352.7	96; 93
17	24.608	16.87	tetradecanoic acid, 2-hydroxy-, methyl ester (or methyl 2-hydroxy tetradecanoate)	258.4	93
18	25.095	1.66	tetracosane; heptadecane, 9-octyl-; tricosane, 2-methyl-	338.7; 352.7; 338.7	93; 93; 86
19	25.309	1.26	1,2-tetradecanediol	230.4	64
20	25.538	2.35	squalene	410.7	98
21	25.592	1.21	pentacosane, 13-undecyl-; heneicosane, 3-methyl-	507; 310.6	52; 38
22	25.708	0.90	octacosane; hexacosane	394.8; 366.7	99; 98
23	26.025	14.37	1,2-tetradecanediol	230.4	90
28	27.252	1.13	$\gamma$ -tocopherol	416.7	98
29	27.554	1.23	fumaric acid, 3,5-difluorophenyl dodecyl ester; Z-14-nonacosane	396.5; 406.8	68; 64
30	27.607	3.19	octacosyl trifluoroacetate; tetratriacontyl pentafluoropropionate	506.8; 640.9	38; 38
31	27.992	5.56	vitamin E; dl- $\alpha$ -tocopherol	430.7; 430.7	99; 99
33	29.112	1.74	campesterol	400.7	62
34	30.173	8.83	$\gamma$ -sitosterol; $\beta$ -sitosterol	414.7; 414.7	99; 95
35	31.166	1.59	2-ethylacridine	207.3	90

Rt: retention time; MW: molecular weight; Qual: percentage of similarity between the molecules present in the sample and those registered in the NIST11 library. When more than one possible assignment is indicated, MW and Qual values for each of the compounds are separated by a semicolon.

Upon conjugation with COS, a synergistic behavior was observed for all phytochemicals. The best results against *X. ampelinus* were attained with the COS–flower extract conjugate complex (MIC = 250  $\mu\text{g}\cdot\text{mL}^{-1}$ ), comparable to those attained for the COS–tetradecanoic acid, COS–linolenic acid and COS–vitamin E conjugate complexes, while the effectiveness of the COS–leaf extract was lower (MIC = 500  $\mu\text{g}\cdot\text{mL}^{-1}$ ). In the case of *E. amylovora*, the COS–flower extract conjugate complex was more effective than the leaf-based one (MIC = 500  $\mu\text{g}\cdot\text{mL}^{-1}$  vs. 750  $\mu\text{g}\cdot\text{mL}^{-1}$ , respectively), but less effective than the COS–tetradecanoic acid, COS–linolenic acid and COS–vitamin E conjugate complexes (MIC = 250  $\mu\text{g}\cdot\text{mL}^{-1}$ , similar to those observed against *X. ampelinus*).

### 2.5.2. In Vitro Antifungal Activity

The results from the *D. seriata* mycelial growth inhibition tests are shown in Figures 2 and S5. At the highest dose (1500  $\mu\text{g}\cdot\text{mL}^{-1}$ ), the flower and the leaf extracts resulted in 82% and 71% inhibition, respectively, while full inhibition was attained at 750  $\mu\text{g}\cdot\text{mL}^{-1}$  for tetradecanoic acid, linolenic acid and vitamin E constituents, and at 250  $\mu\text{g}\cdot\text{mL}^{-1}$  for  $\beta$ -sitosterol. In the case of eicosane, 93% inhibition was observed at the highest dose.

The formation of conjugate complexes improved the activity in all cases, with remarkable improvements in COS–tetradecanoic and COS–linolenic (from 750 down to 187.5  $\mu\text{g}\cdot\text{mL}^{-1}$ ). Concerning flower and leaf extracts, full inhibition was attained at 1000  $\mu\text{g}\cdot\text{mL}^{-1}$  in both cases.

Determination of EC<sub>50</sub> and EC<sub>90</sub> values (50% and 90% maximal effective concentration, respectively), summarized in Table 6, and calculation of synergy factors, presented in Table 7, confirmed the strong synergistic behavior previously mentioned for COS and tetradecanoic and linolenic acids (with SFs of 4.55 and 5.75 for the EC<sub>90</sub>, respectively). In all the other cases, SFs > 1 (i.e., indicative of a synergistic behavior) were also obtained, albeit more moderate.

**Table 4.** Main compounds identified in *L. binervosum* leaf hydromethanolic extract by GC-MS.

Peak	R <sub>t</sub> (min)	Area (%)	Assignment	MW (Da)	Qual
1	17.154	5.41	bicyclo[3.1.1]heptane, 2,6,6-trimethyl-, (1 $\alpha$ ,2 $\beta$ ,5 $\alpha$ ) (also named (-)- <i>trans</i> -pinane); 3-octadecyne	138.3; 250.5	64;58
4	17.593	2.20	cyclohexanol, 1-ethynyl-; phytol, acetate; 1-hexadecyne	124.2; 338.6; 222.4	38; 38; 38
5	18.026	9.83	hexadecanoic acid, methyl ester	270.5	99
6	18.386	4.25	<i>n</i> -hexadecanoic acid; <i>n</i> -decanoic acid	256.4; 172.3	99; 90
7	19.667	7.63	9,12-octadecadienoic acid (Z,Z)-, methyl ester	294.5	99
8	19.740	22.26	9,12,15-octadecatrienoic acid, methyl ester, (Z,Z,Z)-; 9,12,15-octadecatrienoic acid, (Z,Z,Z)-	292.5; 278.4	99; 95
9	19.832	3.80	phytol	296.5	98
12	25.538	1.08	squalene	410.7	99
13	25.962	2.82	nonacosane; eicosane; docosane	408.8; 282.5; 310.6	99; 98; 96
14	26.415	1.77	$\delta$ -tocotrienol (or 2H-1-benzopyran-6-ol, 3,4-dihydro-2,8-dimethyl-2-(4,8,12-trimethyltridecyl)-, [2R-[2*(4R*,8R*)]]-)	396.6	98
15	27.125	1.14	$\beta$ -tocopherol	416.7	99
16	27.252	1.84	$\gamma$ -tocopherol; $\beta$ -tocopherol; $\delta$ -tocopherol, o-methyl-	416.7; 416.7; 416.7	97; 94; 94
17	27.476	1.21	eicosane; octadecane	282.5; 254.5	96; 96
18	27.607	1.57	1H-indole-2-carboxylic acid, 6-(4-ethoxyphenyl)-3-methyl-4-oxo-4,5,6,7-tetrahydro-, isopropyl ester; <i>n</i> -methyl-1-adamantaneacetamide	355.4; 207.31	40; 38
19	27.987	8.08	$\alpha$ -tocopherol	416.7	99
20	28.070	1.35	phytol, acetate; 2-(4-fluoro-phenyl)-4-(3-methyl-benzylidene)-4h-oxazol-5-one	338.6; 281.3	49; 43
21	30.163	19.15	$\gamma$ -sitosterol; $\beta$ -sitosterol	414.7; 414.7	99; 99

Rt: retention time; MW: molecular weight; Qual: percentage of similarity between the molecules present in the sample and those registered in the NIST11 library. When more than one possible assignment is indicated, MW and Qual values for each of the compounds are separated by a semicolon.

**Table 5.** Antibacterial activity of chitosan oligomers (COS), *L. binervosum* flower and leaf hydromethanolic extracts, their main constituents (eicosane, tetradecanoic acid, linolenic acid,  $\beta$ -sitosterol and vitamin E), and their corresponding conjugate complexes (COS–flower extract, COS–leaf extract, COS–eicosane, COS–tetradecanoic acid, COS–linolenic acid, COS– $\beta$ -sitosterol and COS–vitamin E) against the two phytopathogenic bacteria under study at different concentrations (expressed in  $\mu\text{g}\cdot\text{mL}^{-1}$ ).

Pathogen	Compound	Concentration ( $\mu\text{g}\cdot\text{mL}^{-1}$ )									
		62.5	93.75	125	187.5	250	375	500	750	1000	1500
<i>X. ampelinus</i>	COS	+	+	+	+	+	+	+	+	+	–
	Flower extract	+	+	+	+	+	+	+	+	+	–
	Leaf extract	+	+	+	+	+	+	+	+	+	–
	Eicosane	+	+	+	+	+	+	+	+	–	–
	$\beta$ -sitosterol	+	+	+	+	+	+	+	+	–	–
	Tetradecanoic acid	+	+	+	+	+	+	–	–	–	–
	Linolenic acid	+	+	+	+	+	+	–	–	–	–
	Vitamin E	+	+	+	+	+	+	–	–	–	–
	COS–flower extract	+	+	+	+	–	–	–	–	–	–
	COS–leaf extract	+	+	+	+	+	+	+	–	–	–
	COS–eicosane	+	+	+	+	+	+	+	–	–	–
	COS– $\beta$ -sitosterol	+	+	+	+	+	+	–	–	–	–
	COS–tetradecanoic acid	+	+	+	+	–	–	–	–	–	–
	COS–linolenic acid	+	+	+	+	–	–	–	–	–	–
	COS–vitamin E	+	+	+	+	–	–	–	–	–	–
<i>E. amylovora</i>	COS	+	+	+	+	+	+	+	+	+	–
	Flower extract	+	+	+	+	+	+	+	+	+	–
	Leaf extract	+	+	+	+	+	+	+	+	+	–
	Eicosane	+	+	+	+	+	+	+	+	+	+
	$\beta$ -sitosterol	+	+	+	+	+	+	+	+	+	–
	Tetradecanoic acid	+	+	+	+	+	+	–	–	–	–
	Linolenic acid	+	+	+	+	+	+	–	–	–	–
	Vitamin E	+	+	+	+	+	+	–	–	–	–
	COS–flower extract	+	+	+	+	+	+	–	–	–	–
	COS–leaf extract	+	+	+	+	+	+	+	–	–	–
	COS–eicosane	+	+	+	+	+	+	+	+	+	–
	COS– $\beta$ -sitosterol	+	+	+	+	+	–	–	–	–	–
	COS–tetradecanoic acid	+	+	+	+	–	–	–	–	–	–
	COS–linolenic acid	+	+	+	+	–	–	–	–	–	–
	COS–vitamin E	+	+	+	+	–	–	–	–	–	–

“+” and “–” indicate presence and absence of bacterial growth, respectively.

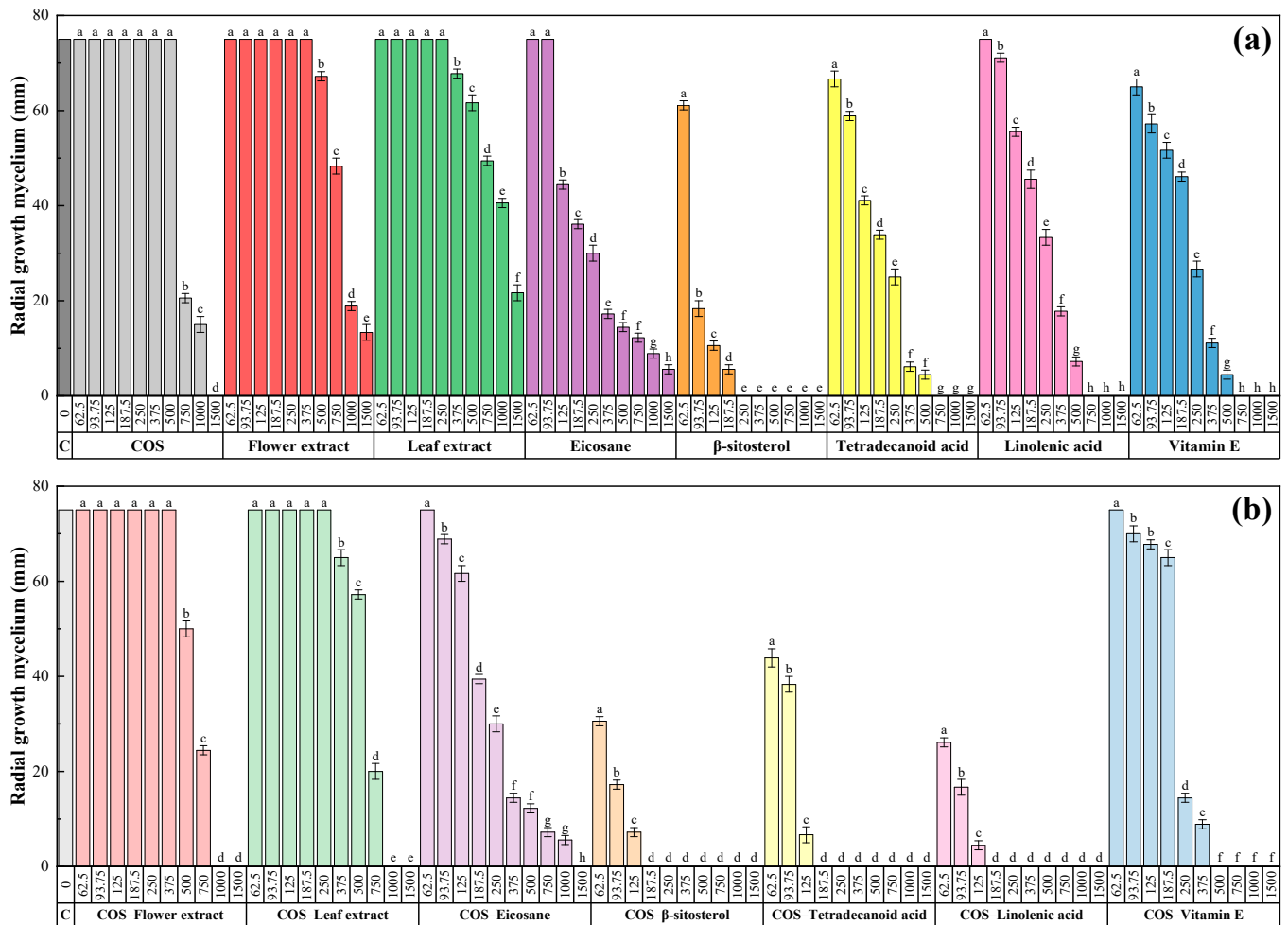


**Figure 2.** Radial growth of the mycelium for *D. seriata* in in vitro tests conducted in PDA medium with different concentrations (62.5, 93.75, 125, 187.5, 250, 375, 500, 750, 1000 and 1500  $\mu\text{g}\cdot\text{mL}^{-1}$ ) of chitosan oligomers (COS), *L. binervosum* flower and leaf extracts, and their main phytochemical constituents (a), and their respective conjugate complexes (b). The same letters above concentrations mean that they are not significantly different at  $p < 0.05$ . Error bars represent standard deviations.

**Table 6.**  $\text{EC}_{50}$  and  $\text{EC}_{90}$  effective concentrations for the different treatments, expressed in  $\mu\text{g}\cdot\text{mL}^{-1}$ .

EC	COS	Flower Extract	Leaf Extract	Eicosane	$\beta$ -Sitosterol	Tetradecanoic	Linolenic	Vitamin E
$\text{EC}_{50}$	744 $\pm$ 42	845 $\pm$ 19	1033 $\pm$ 107	154 $\pm$ 29	82 $\pm$ 11	153 $\pm$ 17	227 $\pm$ 17	212 $\pm$ 13
$\text{EC}_{90}$	1180 $\pm$ 46	1555 $\pm$ 71	2167 $\pm$ 215	1023 $\pm$ 96	151 $\pm$ 26	394 $\pm$ 49	538 $\pm$ 73	434 $\pm$ 57
EC	COS-Flower Extract	COS-Leaf Extract	COS-Eicosane	COS- $\beta$ -Sitosterol	COS-Tetradecanoic	COS-Linolenic	COS-Vitamin E	
$\text{EC}_{50}$		611 $\pm$ 33	625 $\pm$ 20	234 $\pm$ 13	51 $\pm$ 2	109 $\pm$ 2	39 $\pm$ 1	217 $\pm$ 7
$\text{EC}_{90}$		914 $\pm$ 75	966 $\pm$ 64	678 $\pm$ 54	124 $\pm$ 4	130 $\pm$ 4	129 $\pm$ 8	406 $\pm$ 10

**Table 7.** Synergy factors, estimated according to Wadley’s method, for the conjugate complexes under study.

EC	COS-Flower Extract	COS-Leaf Extract	COS-Eicosane	COS- $\beta$ -Sitosterol	COS-Tetradecanoic	COS-Linolenic	COS-Vitamin E
$\text{EC}_{50}$	1.30	1.38	1.09	2.90	2.33	8.98	1.52
$\text{EC}_{90}$	1.47	1.58	1.63	2.15	4.55	5.75	1.56

### 3. Discussion

#### 3.1. Elemental Analysis and Calorific Values Calculation

In relation to the elemental analysis results, the carbon content is close to that reported by Park et al. [24] for *L. tetragonum* (Thunb.) Bullock (45.5%), while the nitrogen content in leaves is in good agreement with that reported for *L. echioides* (L.) Mill. (ca. 2.4%) for complete shoots [25]. The fact that the values of the C/N ratios for flowers are twice those obtained for leaves is consistent with the higher percentage of carbonitrogenated compounds in leaves (viz. *n*-methyl-1-adamantaneacetamide, and 2-(4-fluoro-phenyl)-4-(3-methyl-benzylidene)-4h-oxazol-5-one, which account for ca. 3% according to GC–MS results) than in flowers (viz. 2-ethylacridine, 1.59%).

The calorific values obtained from elemental analysis data, below the 18.82 kJ·g<sup>-1</sup> limit required in EN 14961-2 [26], and the high ash contents (above the 2% limit), preclude the valorization of this halophyte as solid biofuel. Nonetheless, it is worth noting that the fatty acid profile (discussed below), rich in linolenic and linoleic acids, can make *L. binervosum* a promising biofuel feedstock, according to Patel et al. [27].

#### 3.2. Phytochemical Composition

The eicosane content in the flower extract (18%) is higher than the one reported in the aerial parts of *L. leptophyllum* (Schrenk) Kuntze (8%) [28]. Concerning  $\beta$ -sitosterol, its presence was reported in the rhizome of *L. brasiliense* [6], *L. myrianthum* (Schrenk) Kuntze [28], *L. gmelinii* (Willd.) Kuntze and *L. popovii* Kubansk. [29] and in the aerial parts of *L. axillare* (Forssk.) Kuntze [30]. Tetradecanoic, linolenic and linoleic acids were reported in the aerial parts and roots of *L. gmelinii* and *L. popovii* [29], with contents in the 1–4%, 11–27% and 15–32% range, respectively (vs. 22%, 22% and 8%, respectively, for *L. binervosum*).

Although flavonol myricetin (3,5,7-trihydroxy-2-(3,4,5-trihydroxyphenyl)-4-chromenone), reported for *L. aureum* [7] and *L. delicatulum* [8], was not found among the phytochemicals identified by GC–MS in our experimental conditions, significant amounts (7–13%) of antioxidants alternative to myricetin, such as the  $\alpha$ -,  $\beta$ -,  $\gamma$ - and  $\delta$ -tocopherols (e.g., 2-[(4R,8R)-4,8,12-trimethyltridecyl]-3,4-dihydrochromen-6-ol natural vitamin E constituents) were identified. This feature is important because in the literature [31,32] some antimicrobial activity was advocated for myricetin analogs, and a synergistic antioxidant effect of  $\alpha$ -tocopherol and myricetin was described [33].

Concerning the TPC of the flower extract (162 mg GAE/g DW), it was higher than those reported for *L. sinuatum* (L.) Mill. flowers (23–34 mg GAE/g DW) [34,35], but lower than those reported for *L. algarvensis* flower methanol extract (228 mg GAE/g DW) [5]. In regards to the TPC in the leaf extract (58 mg GAE/g DW), it was similar to those reported for *L. delicatulum* shoot extracts (47 mg GAE/g DW) [36]: *L. densiflorum* (Guss.) Kuntze shoots (50–56 mg GAE/g DW) [37,38], *L. algarvensis* leaves (54 mg GAE/g DW) [5], and *L. morisianum* Arrigoni aerial parts (59 mg GAE/g DW) [39]. These values are in the lower end of the range reported by Senizza et al. [40] and Ruiz-Riaguas et al. [8] for *L. delicatulum*, *L. quesadense*, *L. bellidifolium* (Gouan) Dumort., *L. globuliferum* (Boiss. and Heldr.) Kuntze, *L. gmelinii*, *L. iconicum* (Boiss. and Heldr.) Kuntze, *L. lilacinum* (Boiss. and Balansa) Wagenitz and *L. sinuatum* aerial parts extracts (44–172 mg GAE/g DW).

#### 3.3. Antimicrobial Activity of *Limonium* spp. Extracts

The use of halophytes to obtain bioactive antimicrobial extracts is recent, and the effect of the natural products derived from them was generally evaluated against human pathogens (as in the case of the extracts from *Pistacia atlantica* Desf., *Tamarix gallica* L., *T. articulata* Vahl, *Anabasis articulata* (Forssk.) Moq. or *Suaeda fructicosa* (L.) Forssk. [41–44]), not against phytopathogens.

In the particular case of *Limonium* genus., antimicrobial studies were reported for other species, such as *L. brasiliense* [6], *L. awei* (De Not.) Brullo and Erben [45,46], *L. morisianum* [39], *L. socotranum* (Vierh.) Radcl.-Sm. [47], *L. echioides* [48], *L. densiflorum* [37], *L. delicatulum* [36],

*L. myrianthum*, *L. leptophyllum* and *L. gmelinii* [49], but not for *L. binervosum*, so direct efficacy comparisons are not possible.

Regarding the antibacterial activity, Blainski et al. [6] reported a desirable inhibition of bacterial growth for the ethyl-acetate fraction of ternary extracts of *L. brasiliense* against vancomycin-resistant *Enterococcus faecium*, methicillin-resistant *Staphylococcus aureus* and *Klebsiella pneumoniae*, with MIC values of 19, 39 and 625  $\mu\text{g}\cdot\text{mL}^{-1}$ , respectively. The activity of *L. awei* extracts was reported by Filocamo et al. [45], with MIC and minimum bactericidal concentration (MBC) values ranging from 15.6 to 500  $\mu\text{g}\cdot\text{mL}^{-1}$  and from 500 to 4000  $\mu\text{g}\cdot\text{mL}^{-1}$ , respectively, against Gram-positive bacteria and >2000  $\mu\text{g}\cdot\text{mL}^{-1}$  for Gram-negative bacteria. For the same *Limonium* species, Nostro et al. [46] reported MIC and MBC values ranging from 7.8 to 62.5  $\mu\text{g}\cdot\text{mL}^{-1}$  and from 500 to 2000  $\mu\text{g}\cdot\text{mL}^{-1}$ , respectively, against *S. aureus* (including methicillin-resistant strains). Recently, Mandrone et al. [39] found potent anti-staphylococcal properties for *L. morisianum* extract, with an average  $\text{IC}_{50}$  value of 9.2 [6.8–12.3]  $\mu\text{g}\cdot\text{mL}^{-1}$ . Moreover, recently, Al-Madhagi et al. [47] noted that methanol leaf and flower extracts from *L. socotranum* exhibited higher antibacterial activity against *Micrococcus luteus* (MIC 15.6  $\mu\text{g}\cdot\text{mL}^{-1}$ ), *S. aureus* (MIC 125  $\mu\text{g}\cdot\text{mL}^{-1}$ ) and *Pseudomonas aeruginosa* (MIC 125  $\mu\text{g}\cdot\text{mL}^{-1}$ ) than stem extracts.

Concerning the antifungal activity of *Limonium* spp., a low antifungal activity was reported for *L. echioides* (against *Fusarium oxysporum* and *Penicillium* sp. [48]), for *L. awei* (against *Candida albicans* [46]), and for *L. densiflorum* and *L. delicatilum* (against *Candida* spp. [36,37]). Nonetheless, a stronger antifungal activity against *C. albicans* and *Aspergillus niger*, with full inhibition at concentrations as low as 62 and 125  $\mu\text{g}\cdot\text{mL}^{-1}$ , respectively, were found for *L. socotranum* leaf and flower extracts [47]. Significant antifungal activities against *C. glabrata*, with  $\text{IC}_{50}$  values in the 4.96–6.83  $\mu\text{g}\cdot\text{mL}^{-1}$ , were also reported for secondary metabolites from *L. myrianthum*, *L. leptophyllum* and *L. gmelinii* by Gadetskaya et al. [49].

### 3.4. Antimicrobial Activity of the Main Identified Phytochemicals

All the main phytochemicals found in the *L. binervosum* flower and leaf extracts have been reported to have both antimicrobial and antifungal activity (albeit not against any of the phytopathogens referred herein).

Eicosane is effective against bacteria such as *Escherichia coli*, *Salmonella typhi* and *S. aureus* [50], and against fungi such as *Rhizoctonia solani* [51]. Likewise, the antimicrobial activity of  $\beta$ -sitosterol against both bacteria (*S. typhi*, *Corynebacterium diphtheriae*, *Bacillus subtilis*, *Shigella dysenteriae* and *Vibrio cholerae*) and fungi (*Fusarium* spp. and *Penicillium* spp.) was reported by Kiprono et al. [52].

Concerning fatty acids, which are the major constituents of *L. binervosum* extracts, it was demonstrated that the antibacterial action of long-chain unsaturated fatty acids is mediated by the inhibition of fatty acid synthesis [53], and it was shown that both saturated and unsaturated fatty acids have antifungal activity, although saturated fatty acids would show a stronger activity [54]. In particular, antimicrobial properties of tetradecanoic acid were referred to in the literature (against, for instance, *Listeria monocytogenes* [55] and *C. albicans* [56]), as well as for its derivatives, such as methyl 2-hydroxytetradecanoate (against *C. albicans*, *Cryptococcus neoformans* and *A. niger* [57]). Regarding linolenic acid, Lee et al. [58] concluded that this fatty acid has a strong antibacterial activity against *B. cereus* and *S. aureus*, and Walters et al. [59] showed its activity against *R. solani*, *Pythium ultimum*, *Pyrenophora avenae* and *Crinipellis perniciosa*.

With regard to vitamin E, its antibacterial activity against *E. coli*, *S. aureus*, *S. epidermidis*, *P. aeruginosa*, *Proteus* spp., *Klebsiella* spp., and *Enterobacter* spp. was evidenced by Al-Salih et al. [60], and it was reported that—in combination with fluconazole—it results effective in the treatment of some human fungal diseases [61].

### 3.5. On the Synergistic Behavior Observed for the Conjugate Complexes

The combination of chitosan with several of the main constituents of *L. binervosum* extracts has precedents in the literature. For instance, combinations of chitosan with vitamin

E were studied by Yeamsuksawat and Liang [62], Martins et al. [63] and Raza et al. [64]. The rationale behind such choice is that, while  $\alpha$ -tocopherol has feeble stability, it is improved by encapsulation in chitosan as a capping agent, as well as its release when required over a sustained period. Similarly, Liu et al. [65] reported the formation of self-assembled nanoparticles by coupling chitosan with linolenic acid, taking advantage of the fact that chitosan is known to inhibit the linoleic (and linolenic) acid oxidation process [66]. In the case of tetradecanoic acid, chitosan–tetradecanoic acid nanogels with MIC values of  $10 \text{ mg}\cdot\text{mL}^{-1}$  against *S. enterica* were reported by Rajaei et al. [67].

Nonetheless, none of the aforementioned combinations are conjugated complexes, and the existence of interactions between the two components in terms of antimicrobial activity was not explored. Albeit for other phytochemicals different from the ones present in *L. binervosum*, a synergistic behavior upon conjugation with COS was reported in the literature against phytopathogens: e.g., for horsetail (*Equisetum arvense* L.) and nettle (*Urtica dioica* L.) extracts against eight fungal species involved in grapevine trunk diseases [68], with  $\text{EC}_{90}$  values in the  $208\text{--}1000 \text{ }\mu\text{g}\cdot\text{mL}^{-1}$  range (depending on the extract and on the *Botryosphaeriaceae* taxa). The value reported in this work for the COS–flower extract complex ( $914 \text{ }\mu\text{g}\cdot\text{mL}^{-1}$ ) would be on the upper limit.

For the same phytopathogens studied herein, and also for extracts from halophytes, MIC values of 375 and  $500 \text{ }\mu\text{g}\cdot\text{mL}^{-1}$  against *X. ampelinus* and 187.5 and  $500 \text{ }\mu\text{g}\cdot\text{mL}^{-1}$  against *E. amylovora* were found for the conjugate complexes formed between COS and rock samphire (*Crithmum maritimum* L.) and sea carrot (*Daucus carota* subsp. *gummifer* (Syme) Hook.fil.) hydromethanolic extracts, respectively. Such inhibition values are worse than the one reported herein against *X. ampelinus* for the COS–flower extract conjugate complex (MIC =  $250 \text{ }\mu\text{g}\cdot\text{mL}^{-1}$ ), but slightly better than/comparable to that obtained against *E. amylovora* (MIC =  $500 \text{ }\mu\text{g}\cdot\text{mL}^{-1}$ ) [69].

The mechanism of synergistic action of such COS–phytochemical conjugates has not been elucidated yet. Nonetheless, it was suggested that it might be the result of an enhanced additive antimicrobial effect, per se, and/or via a concurrent action on diverse microbial metabolic sites. An increase in the cationic surface charge of COS may also result from conjugation with phytochemicals, which would enhance the linkage to negatively charged site-specific binding receptors on the bacterial/fungal membranes [70–73].

## 4. Material and Methods

### 4.1. Reagents

High-molecular weight (310,000–375,000 Da) chitosan (CAS 9012-76-4) was purchased from Hangzhou Simit Chem. and Tech. Co. (Hangzhou, China). Neutrase™ 0.8 L enzyme was obtained from Novozymes A/S (Bagsværd, Denmark). The preparation of chitosan oligomers (COS) was carried out according to the procedure reported by Santos-Moriano et al. [74], with the modifications indicated in [73].

Eicosane (CAS 112-95-8, 99%), 1,2-tetradecanoic acid (CAS 544-63-8, Sigma Grade,  $\geq 99\%$ ), linolenic acid (CAS 463-40-1,  $\geq 99\%$ ),  $\beta$ -sitosterol (CAS 83-46-5, analytical standard), vitamin E ( $\alpha$ -tocopherol, CAS 10191-41-0, analytical standard), methanol (CAS 67-56-1, UHPLC, suitable for MS), tryptic soy broth (TSB, CAS 8013-01-2) and tryptic soy agar (TSA, CAS 91079-40-2) were supplied by Sigma-Aldrich (Madrid, Spain). Potato dextrose agar (PDA) was acquired from Becton Dickinson (Bergen County, NJ, USA). All reagents were used as supplied without further purification.

### 4.2. Plant Material and Extraction Procedure

*L. binervosum* was collected in sea cliffs in Llanes (Asturias, Spain;  $43^{\circ}26'10.7''$  N  $4^{\circ}49'25.1''$  W) in early September 2020. Separate composite samples of flowers and leaves were obtained by thoroughly mixing the aerial parts from different specimens ( $n = 15$ ). The composite samples were shade-dried, pulverized in a mechanical grinder, homogenized and sieved (1 mm mesh).

*L. binervosum* flower samples were mixed (1:20 *w/v*) with a 1:1 *v/v* methanol:water solution and heated for 30 min in a water bath at 50 °C. Subsequently, they were sonicated for 5 min in pulse mode with a 1 min stop for each 2.5 min, using a Hielscher Ultrasonics (Teltow, Germany) probe-type ultrasonicator (model UIP1000hdT; 1000 W, 20 kHz). The solution was subjected to centrifugation at 9000 rpm for 15 min, and the supernatant was filtered through Whatman No. 1 paper. Aliquots were lyophilized for CHNS and FTIR analyses. The extraction procedure for leaf samples was identical.

Each extraction procedure was replicated three times (on subsamples of the flower and leaf composite samples), and the resulting hydromethanolic extracts were mixed to obtain the samples for GC-MS analysis.

#### 4.3. Bacterial and Fungal Isolates

The *X. ampelinus* and *E. amylovora* bacterial isolates were supplied by CECT (Valencia, Spain), with CCUG 21976 and NCPPB 595 strain designations, respectively. *D. seriata* (isolate Y-084-01-01a, code ITACYL\_F098), obtained from “Tempranillo” grapevine plants from P.D.O. Toro (Spain), was supplied by ITACYL (Valladolid, Spain) [75] as a lyophilized vial, which was reconstituted and refreshed as a PDA subculture.

#### 4.4. Physicochemical Characterization

Elemental analyses of dry ground samples (3 mg/sample) were performed with a CHNS-932 apparatus (LECO, St. Joseph, MI, USA).

Calorific values were calculated from elemental analysis data according to Talwalkar et al. [76], using the following equation:

$$\text{HHV} = (0.341 \times \%C) + (1.322 \times \%H) - 0.12 (\%O + \%N), \quad (1)$$

where HHV is the heating value for the dry material, expressed in  $\text{kJ}\cdot\text{g}^{-1}$ , and %C, %H, %O and %N are the mass fractions, expressed in wt% of dry material.

Thermal gravimetric (TGA) and differential scanning calorimetry (DSC) analyses were conducted with a simultaneous TG-DSC2 apparatus (Mettler Toledo; Columbus, OH, USA). Samples (10 mg/sample) were heated from 30 to 600 °C under  $\text{N}_2:\text{O}_2$  (4:1) flow ( $20 \text{ cm}^3\cdot\text{min}^{-1}$ ), at a  $20 \text{ }^\circ\text{C}\cdot\text{min}^{-1}$  heating rate.

The infrared spectra were obtained with a Nicolet iS50 Fourier-transform infrared spectrometer (Thermo Scientific; Waltham, MA, USA), equipped with an in-built diamond attenuated total reflection (ATR) system. A spectral resolution of  $1 \text{ cm}^{-1}$  over the  $400\text{--}4000 \text{ cm}^{-1}$  range was used, taking the interferograms that resulted from co-adding 64 scans.

The colorimetric quantification of the total polyphenol content (TPC), expressed in gallic acid equivalents (GAE), was conducted according to the procedure described in [77], using a UV-Vis Cary 100 spectrometer (Agilent Technologies; Santa Clara, CA, USA).

The gas chromatography–mass spectrometry (GC–MS) analyses of the hydroalcoholic plant extracts (obtained as a mixture of three extractions) were carried out at the Research Support Services (STI) at Universidad de Alicante (Alicante, Spain). A model 7890A gas chromatograph coupled to a model 5975C quadrupole mass spectrometer (Agilent Technologies). The chromatographic conditions were: 3 injections/vial; 1  $\mu\text{L}$  injection volume; 280 °C injector temperature, in splitless mode; the 60 °C initial oven temperature was held for 2 min, followed by a  $10 \text{ }^\circ\text{C}\cdot\text{min}^{-1}$  ramp up to a 300 °C final temperature, kept for 15 min. The chromatographic column used for the separation of the compounds was an HP-5MS UI (Agilent Technologies) of 30 m length, 0.250 mm diameter and 0.25  $\mu\text{m}$  film. The MS conditions were: temperature of the electron impact source of the mass spectrometer = 230 °C and of the quadrupole = 150 °C; 70 eV ionization energy. Equipment calibration was conducted using test mixture 2 for apolar capillary columns according to Grob (Supelco 86501) and PFTBA tuning standards. Compound identification was carried out using the NIST11 library [78].

#### 4.5. In Vitro Antibacterial Activity Assessment

The antibacterial activity was assessed by determining the minimum inhibitory concentration (MIC). The agar dilution method was used, according to CLSI standard M07-11 [79]. An isolated colony of *X. ampelinus* was incubated in TSB liquid medium at 26 °C for 18 h. Starting from a  $10^8$  CFU·mL<sup>-1</sup> concentration, serial dilutions were then conducted to obtain a final inoculum of  $\sim 10^4$  CFU·mL<sup>-1</sup>. Subsequently, bacterial suspensions were delivered to the surface of TSA plates amended with the treatments at concentrations ranging from 62.5 to 1500 µg·mL<sup>-1</sup>. The plates were incubated at 26 °C for 24 h. The procedure for *E. amylovora* was identical, except for the incubation temperature (30 °C). MICs were visually determined as the lowest concentrations at which no bacterial growth was visible in the agar dilutions. All experiments were run in triplicate, with each replicate consisting of 3 plates per treatment/concentration.

#### 4.6. In Vitro Antifungal Activity Assessment

The antifungal activity of the different treatments was determined according to EUCAST standard antifungal susceptibility testing procedures [80], using the agar dilution method. Aliquots of stock solutions were incorporated onto the PDA medium to obtain concentrations in the 62.5–1500 µg·mL<sup>-1</sup> range. Mycelial plugs (5 mm in diameter), taken from the margin of 7-day-old *D. seriata* PDA cultures, were transferred to plates amended with aforementioned concentrations of each treatment (3 plates per treatment/concentration, with 2 replicates). Plates were incubated in the dark at 25 °C for 7 days. PDA medium without any amendment was used as the control. Mycelial growth inhibition was estimated according to the formula:

$$((d_c - d_t) / d_c) \times 100, \quad (2)$$

where  $d_c$  and  $d_t$  represent the average diameters of the fungal colony of the control and of the treated fungal colony, respectively. EC<sub>50</sub> and EC<sub>90</sub> effective concentrations were estimated in IBM SPSS Statistics v.25 (IBM; Armonk, NY, USA) software using PROBIT analysis. The level of interaction was determined according to Wadley's method [81].

#### 4.7. Statistical Analysis

Given that the homogeneity and homoscedasticity requirements were satisfied (according to Shapiro–Wilk and Levene tests, respectively), the mycelial growth inhibition results for *D. seriata* were statistically analyzed in IBM SPSS Statistics v.25 software using one-way analysis of variance (ANOVA), followed by post hoc comparison of means through Tukey's test at  $p < 0.05$ .

## 5. Conclusions

A halophyte from the cliffs of the Atlantic coasts of Europe, viz. *Limonium binervosum* (rock sea-lavender) was studied by elemental and thermal analysis, FTIR spectroscopy and GC–MS with a view to its valorization. The use of its biomass as a solid biofuel can be ruled out, given that its higher heating value (in the 16–18 kJ·g<sup>-1</sup> range) and content of ashes (5.6% and 17% for flowers and leaves, respectively) do not meet the minimum legal requirements, but its high content in fatty acids open the door to potential exploitation as a biofuel feedstock. Another potential application would be related to the use of its hydrometanolic extracts as natural biocontrol products, given that phytochemicals with antimicrobial properties were found in significant amounts: both flower and leaf extracts contained eicosane (4–18%), β-sitosterol (9–19%) and tocopherols (7–13%), besides fatty acids and their esters (22% of tetradecanoic acid in the flower extract, and 30% of linolenic and linoleic acids in the leaf extract). The inhibitory activity of the extracts and their main constituents, alone or in combination with chitosan oligomers, was tested in vitro against *X. ampelinus*, *E. amylovora* and *D. seriata* phytopathogens. A remarkable antibacterial activity was observed against *X. ampelinus* (with a MIC value of 250 µg·mL<sup>-1</sup>) and *E. amylovora* (MIC = 500 µg·mL<sup>-1</sup>) for the conjugated complex of the flower extract with COS, which also resulted in an EC<sub>90</sub> of 914 µg·mL<sup>-1</sup> against *D. seriata*. In view of these results, the

conjugate complexes of this halophyte may be put forward as promising antimicrobial treatments for apple tree and grapevine diseases in organic agriculture.

**Supplementary Materials:** The following are available online at <https://www.mdpi.com/article/10.3390/plants10091852/s1>, Figure S1: TG, DTG and DSC curves for *L. binervosum* flowers, Figure S2: TG, DTG and DSC curves for *L. binervosum* leaves, Figure S3: GC–MS spectrum of *L. binervosum* flower hydromethanolic extract, Figure S4: GC–MS spectrum of *L. binervosum* leaf hydromethanolic extract, Figure S5: Growth inhibition of *D. seriata* for the conjugate complexes under study, Table S1: GC-MS results for the *L. binervosum* flower hydromethanolic extract, Table S2: GC-MS results for the *L. binervosum* leaf hydromethanolic extract.

**Author Contributions:** Conceptualization, J.M.-G. and P.M.-R.; methodology, B.L.-V. and J.C.-G.; validation, B.L.-V., J.C.-G. and J.M.-G.; formal analysis, J.C.-G. and P.M.-R.; investigation, E.S.-H., L.B.-D., N.L.-L., J.C.-G., B.L.-V., J.M.-G. and P.M.-R.; resources, J.M.-G. and P.M.-R.; writing—original draft preparation, E.S.-H., L.B.-D., N.L.-L., J.C.-G., B.L.-V., J.M.-G. and P.M.-R.; writing—review and editing, P.M.-R.; visualization, E.S.-H. and L.B.-D.; supervision, P.M.-R.; project administration, J.M.-G. and P.M.-R.; funding acquisition, J.M.-G. and P.M.-R. All authors have read and agreed to the published version of the manuscript.

**Funding:** This research was funded by Junta de Castilla y León under project VA258P18, with FEDER co-funding, by Cátedra Agrobank under “IV Convocatoria de Ayudas de la Cátedra AgroBank para la transferencia del conocimiento al sector agroalimentario” program; by Fundación Ibercaja-Universidad de Zaragoza under the “Convocatoria Fundación Ibercaja-Universidad de Zaragoza de proyectos de investigación, desarrollo e innovación para jóvenes investigadores” program.

**Institutional Review Board Statement:** Not applicable.

**Informed Consent Statement:** Not applicable.

**Data Availability Statement:** The data presented in this study are available on request from the corresponding author. The data are not publicly available due to their relevance to be part of an ongoing Ph.D. Thesis.

**Acknowledgments:** The authors gratefully acknowledge the support of Pilar Blasco and Pablo Candela at the Servicios Técnicos de Investigación, Universidad de Alicante, for conducting the GC–MS analyses.

**Conflicts of Interest:** The funders had no role in the design of the study; in the collection, analyses, or interpretation of data; in the writing of the manuscript, or in the decision to publish the results.

## References

1. Caperta, A.D.; Castro, S.; Loureiro, J.; Róis, A.; Conceição, S.; Costa, J.; Rhazi, L.; Santo, D.E.; Arsénio, P. Biogeographical, ecological and ploidy variation in related asexual and sexual *Limonium taxa* (Plumbaginaceae). *Bot. J. Linn. Soc.* **2016**, *183*, 75–93. [[CrossRef](#)]
2. Lledó, M.D.; Crespo, M.B.; Fay, M.F.; Chase, M.W. Molecular phylogenetics of *Limonium* and related genera (Plumbaginaceae): Biogeographical and systematic implications. *Am. J. Bot.* **2005**, *92*, 1189–1198. [[CrossRef](#)] [[PubMed](#)]
3. Salmon, C.E. *Limonium binervosum* Salm. In *Reports of the Botanical Society and Exchange Club; Report for 1922*; Druce, G.C., Ed.; T. Buncle & Co.: Arbroath, UK, 1923; Volume 7, p. 1054.
4. Ingrouille, M.J.; Stace, C.A. The *Limonium binervosum* aggregate (Plumbaginaceae) in the British Isles. *Bot. J. Linn. Soc.* **1986**, *92*, 177–217. [[CrossRef](#)]
5. Rodrigues, M.J.; Soszynski, A.; Martins, A.; Rauter, A.; Neng, N.R.; Nogueira, J.M.; Varela, J.; Barreira, L.; Custódio, L. Unravelling the antioxidant potential and the phenolic composition of different anatomical organs of the marine halophyte *Limonium algarvense*. *Ind. Crop. Prod.* **2015**, *77*, 315–322. [[CrossRef](#)]
6. Blainski, A.; Gionco, B.; Oliveira, A.G.; Andrade, G.; Scarminio, I.S.; Silva, D.B.; Lopes, N.P.; Mello, J.C. Antibacterial activity of *Limonium brasiliense* (Baicuru) against multidrug-resistant bacteria using a statistical mixture design. *J. Ethnopharmacol.* **2017**, *198*, 313–323. [[CrossRef](#)] [[PubMed](#)]
7. Geng, D.; Chi, X.; Dong, Q.; Hu, F. Antioxidants screening in *Limonium aureum* by optimized on-line HPLC–DPPH assay. *Ind. Crop. Prod.* **2015**, *67*, 492–497. [[CrossRef](#)]
8. Ruiz-Riaguas, A.; Zengin, G.; Sinan, K.; Salazar-Mendías, C.; Llorent-Martínez, E. Phenolic Profile, Antioxidant Activity, and Enzyme Inhibitory Properties of *Limonium delicatulum* (Girard) Kuntze and *Limonium quesadense* Erben. *J. Chem.* **2020**, *2020*, 1–10. [[CrossRef](#)]

9. Mutlu-Ingok, A.; Devecioglu, D.; Dikmetas, D.N.; Karbancioglu-Guler, F.; Capanoglu, E. Antibacterial, Antifungal, Antimycotoxic, and Antioxidant Activities of Essential Oils: An Updated Review. *Molecules* **2020**, *25*, 4711. [[CrossRef](#)]
10. Willems, A.; Gillis, M.; Kersters, K.; Broecke, L.V.D.; De Ley, J. Transfer of *Xanthomonas ampelina* Panagopoulos 1969 to a New Genus, *Xylophilus* gen. nov., as *Xylophilus ampelinus* (Panagopoulos 1969) comb. nov. *Int. J. Syst. Bacteriol.* **1987**, *37*, 422–430. [[CrossRef](#)]
11. Szegedi, E.; Civerolo, E.L. Bacterial diseases of grapevine. *Int. J. Hortic. Sci.* **2011**, *17*, 45–49. [[CrossRef](#)]
12. Donat, V.; Biosca, E.; Peñalver, J.; Lopez, M. Exploring diversity among Spanish strains of *Erwinia amylovora* and possible infection sources. *J. Appl. Microbiol.* **2007**, *103*, 1639–1649. [[CrossRef](#)] [[PubMed](#)]
13. Larignon, P.; Fulchic, R.; Cere, L.; Dubos, B. Observation on Black Dead Arm in French Vineyards. *Phytopathol. Mediterr.* **2001**, *40*, 336–342. [[CrossRef](#)]
14. Mondello, V.; Songy, A.; Battiston, E.; Pinto, C.; Coppin, C.; Trotel-Aziz, P.; Clément, C.; Mugnai, L.; Fontaine, F. Grapevine Trunk Diseases: A Review of Fifteen Years of Trials for Their Control with Chemicals and Biocontrol Agents. *Plant Dis.* **2018**, *102*, 1189–1217. [[CrossRef](#)]
15. Stevens, N.E. Two Apple Black Rot Fungi in the United States. *Mycologia* **1933**, *25*, 536–548. [[CrossRef](#)]
16. Brown-Rytlewski, D.E.; McManus, P.S. Virulence of *Botryosphaeria dothidea* and *Botryosphaeria obtusa* on Apple and Management of Stem Cankers with Fungicides. *Plant Dis.* **2000**, *84*, 1031–1037. [[CrossRef](#)]
17. Ii, E.A.B. *Botryosphaeria* Diseases of Apple and Peach in the Southeastern United States. *Plant Dis.* **1986**, *70*, 480. [[CrossRef](#)]
18. Kanakiya, A.; Padalia, H.; Pande, J.; Chanda, S. Physicochemical, phytochemical and pharmacognostic study of *Limonium stocksii*. A halophyte from Gujarat. *J. Phytopharm.* **2018**, *7*, 312–318.
19. da Luz, B.R. Attenuated total reflectance spectroscopy of plant leaves: A tool for ecological and botanical studies. *New Phytol.* **2006**, *172*, 305–318. [[CrossRef](#)] [[PubMed](#)]
20. Socrates, G. *Infrared and Raman Characteristic Group Frequencies: Tables and Charts*, 3rd ed.; Wiley: Chichester, NY, USA, 2001; p. 347.
21. Mot, A.; Silaghi-Dumitrescu, R.; Sarbu, C. Rapid and effective evaluation of the antioxidant capacity of propolis extracts using DPPH bleaching kinetic profiles, FT-IR and UV–vis spectroscopic data. *J. Food Compos. Anal.* **2011**, *24*, 516–522. [[CrossRef](#)]
22. Junior, V.; Arruda, I.; Bemme, L. Caracterização térmica e espectroscópica de microcápsulas de quitosana incorporada de própolis. *Rev. Eletrônica da Univar* **2013**, *2*, 161–165.
23. Silva, A.J.; Silva, J.R.; de Souza, N.; Souto, P.C.D.S. Membranes from latex with propolis for biomedical applications. *Mater. Lett.* **2014**, *116*, 235–238. [[CrossRef](#)]
24. Park, S.-I.; Hwang, Y.-S.; Um, J.-S. Estimating blue carbon accumulated in a halophyte community using UAV imagery: A case study of the southern coastal wetlands in South Korea. *J. Coast. Conserv.* **2021**, *25*, 1–9. [[CrossRef](#)]
25. Ochoa-Hueso, R.; Corona, M.E.P.; Manrique, E. Impacts of Simulated N Deposition on Plants and Mycorrhizae from Spanish Semiarid Mediterranean Shrublands. *Ecosystems* **2013**, *16*, 838–851. [[CrossRef](#)]
26. Duca, D.; Riva, G.; Pedretti, E.F.; Toscano, G. Wood pellet quality with respect to EN 14961-2 standard and certifications. *Fuel* **2014**, *135*, 9–14. [[CrossRef](#)]
27. Patel, M.K.; Pandey, S.; Brahmabhatt, H.R.; Mishra, A.; Jha, B. Lipid content and fatty acid profile of selected halophytic plants reveal a promising source of renewable energy. *Biomass Bioenergy* **2019**, *124*, 25–32. [[CrossRef](#)]
28. Gadetskaya, A.; Zhusupova, G.; Ross, S. Composition of the volatile oil from aerial parts of *Limonium* genus. *Chem. J. Kazakhstan* **2015**, *2*, 274–279.
29. Korul’Kina, L.M.; Zhusupova, G.E.; Shul’Ts, E.E.; Erzhanov, K.B. Fatty-acid composition of two *Limonium* plant species. *Chem. Nat. Compd.* **2004**, *40*, 417–419. [[CrossRef](#)]
30. Bashir, A.; Abdalla, A.A.; Wasfi, I.A.; Hassan, E.S.; Amiri, M.H.; Crabb, T.A. Flavonoids of *Limonium axillare*. *Int. J. Pharmacogn.* **1994**, *32*, 366–372. [[CrossRef](#)]
31. Yurchyshyn, O.; Rusko, G.; Kutsyk, R. Antimicrobial effect of south Ukrainian sea lavender *Limonium meyeri* (Boiss.) O. Kuntze and *Limonium hypanicum* Klok. with especial emphasizing against staphylococci and Propionibacteria. *Pharma Innov. J.* **2017**, *6*, 380–384.
32. Taheri, Y.; Suleria, H.A.R.; Martins, N.; Sytar, O.; Beyatli, A.; Yeskaliyeva, B.; Seitimova, G.; Salehi, B.; Semwal, P.; Painuli, S.; et al. Myricetin bioactive effects: Moving from preclinical evidence to potential clinical applications. *BMC Complement. Med. Ther.* **2020**, *20*, 1–14. [[CrossRef](#)]
33. Marinova, E.; Toneva, A.; Yanishlieva, N. Synergistic antioxidant effect of  $\alpha$ -tocopherol and myricetin on the autoxidation of triacylglycerols of sunflower oil. *Food Chem.* **2008**, *106*, 628–633. [[CrossRef](#)]
34. Li, A.-N.; Li, S.; Li, H.-B.; Xu, D.-P.; Xu, X.-R.; Chen, F. Total phenolic contents and antioxidant capacities of 51 edible and wild flowers. *J. Funct. Foods* **2014**, *6*, 319–330. [[CrossRef](#)]
35. Skrajda, M.N. Phenolic compounds and antioxidant activity of edible flowers. *J. Educ. Health Sport* **2017**, *7*, 946–956.
36. Medini, F.; Fellah, H.; Ksouri, R.; Abdelly, C. Total phenolic, flavonoid and tannin contents and antioxidant and antimicrobial activities of organic extracts of shoots of the plant *Limonium delicatulum*. *J. Taibah Univ. Sci.* **2014**, *8*, 216–224. [[CrossRef](#)]
37. Medini, F. Effects of physiological stage and solvent on polyphenol composition, antioxidant and antimicrobial activities of *Limonium densiflorum*. *J. Med. Plants Res.* **2011**, *5*. [[CrossRef](#)]

38. Medini, F.; Bourgou, S.; Lalancette, K.; Snoussi, M.; Mkadmini, K.; Coté, I.; Abdelly, C.; Legault, J.; Ksouri, R. Phytochemical analysis, antioxidant, anti-inflammatory, and anticancer activities of the halophyte *Limonium densiflorum* extracts on human cell lines and murine macrophages. *S. Afr. J. Bot.* **2015**, *99*, 158–164. [[CrossRef](#)]
39. Mandrone, M.; Bonvicini, F.; Lianza, M.; Sanna, C.; Maxia, A.; Gentilomi, G.; Poli, F. Sardinian plants with antimicrobial potential. Biological screening with multivariate data treatment of thirty-six extracts. *Ind. Crop. Prod.* **2019**, *137*, 557–565. [[CrossRef](#)]
40. Senizza, B.; Zhang, L.; Rocchetti, G.; Zengin, G.; Ak, G.; Yildiztugay, E.; Elbasan, F.; Jugreet, S.; Mahomoodally, M.F.; Lucini, L. Metabolomic profiling and biological properties of six *Limonium* species: Novel perspectives for nutraceutical purposes. *Food Funct.* **2021**, *12*, 3443–3454. [[CrossRef](#)]
41. Belyagoubi-Benhammou, N.; Belyagoubi, L.; Gismondi, A.; Di Marco, G.; Canini, A.; Bekkara, F.A. GC/MS analysis, and antioxidant and antimicrobial activities of alkaloids extracted by polar and apolar solvents from the stems of *Anabasis articulata*. *Med. Chem. Res.* **2019**, *28*, 754–767. [[CrossRef](#)]
42. Benmahieddine, A.; Belyagoubi-Benhammou, N.; Belyagoubi, L.; El Zerey-Belaskri, A.; Gismondi, A.; Di Marco, G.; Canini, A.; Bechlaghem, N.; Bekkara, F.A.; Djebli, N. Influence of plant and environment parameters on phytochemical composition and biological properties of *Pistacia atlantica* Desf. *Biochem. Syst. Ecol.* **2021**, *95*, 104231. [[CrossRef](#)]
43. Saïdana, D.; Mahjoub, S.; Boussaada, O.; Chriaa, J.; Mahjoub, M.A.; Chéraif, I.; Daami, M.; Mighri, Z.; Helal, A.N. Antibacterial and antifungal activities of the essential oils of two saltcedar species from Tunisia. *J. Am. Oil Chem. Soc.* **2008**, *85*, 817–826. [[CrossRef](#)]
44. Tabet, A.; Boukhari, A. Antioxidant and antibacterial activities of two Algerian halophytes. *Int. J. Pharm. Sci. Rev. Res.* **2018**, *50*, 114–121.
45. Filocamo, A.; Nostro, A.; Giovannini, A.; Catania, S.; Costa, C.; Marino, A.; Bisignano, G. Antimicrobial activity of *Limonium awei* (De Not.) Brullo & Erben extracts. *Planta Med.* **2010**, *76*, P465. [[CrossRef](#)]
46. Nostro, A.; Filocamo, A.; Giovannini, A.; Catania, S.; Costa, C.; Marino, A.; Bisignano, G. Antimicrobial activity and phenolic content of natural site and micropropagated *Limonium awei* (De Not.) Brullo & Erben plant extracts. *Nat. Prod. Res.* **2011**, *26*, 1–5. [[CrossRef](#)]
47. Al-Madhagi, W.M.; Hashim, N.M.; Ali, N.A.A.; Othman, R. Phytochemical screening, cytotoxic and antimicrobial activities of *Limonium socotranum* and *Peperomia blanda* extracts. *Trop. Biomed.* **2019**, *36*, 11–21.
48. Saidana, D.; Boussaada, O.; Ayed, F.; Mahjoub, M.A.; Mighri, Z.; Helal, A.N. Their vitrofrees radical-scavenging and antifungal activities of the medicinal *Herblimonium Echioides* L. growing wild in Tunisia. *J. Food Process. Preserv.* **2012**, *37*, 533–540. [[CrossRef](#)]
49. Gadetskaya, A.; Mohamed, S.; Tarawneh, A.; Ma, G.; Ponomarev, B.; Zhussupova, G.; Cantrell, C.; Cutler, S.; Ross, S. Biologically potent metabolites from *Limonium* species. *Planta Med.* **2016**, *81*, S1–S381. [[CrossRef](#)]
50. Firdaus, M.; Kartikaningsih, H.; Sulifah, U. *Sargassum* spp extract inhibits the growth of foodborne illness bacteria. *AIP Conf. Proc.* **2019**, *2202*, 020083. [[CrossRef](#)]
51. Ahsan, T.; Chen, J.; Zhao, X.; Irfan, M.; Wu, Y. Extraction and identification of bioactive compounds (eicosane and dibutyl phthalate) produced by *Streptomyces* strain KX852460 for the biological control of *Rhizoctonia solani* AG-3 strain KX852461 to control target spot disease in tobacco leaf. *AMB Express* **2017**, *7*, 54. [[CrossRef](#)]
52. Kiprono, P.C.; Kaberia, F.; Keriko, J.M.; Karanja, J.N. The in vitro Anti-Fungal and Anti-Bacterial Activities of  $\beta$ -Sitosterol from *Senecio lyratus* (Asteraceae). *Z. Naturforsch. C. J. Biosci.* **2000**, *55*, 485–488. [[CrossRef](#)]
53. Zheng, C.J.; Yoo, J.-S.; Lee, T.-G.; Cho, H.-Y.; Kim, Y.-H.; Kim, W.-G. Fatty acid synthesis is a target for antibacterial activity of unsaturated fatty acids. *FEBS Lett.* **2005**, *579*, 5157–5162. [[CrossRef](#)] [[PubMed](#)]
54. Liu, S.; Ruan, W.; Li, J.; Xu, H.; Wang, J.; Gao, Y.; Wang, J. Biological Control of Phytopathogenic Fungi by Fatty Acids. *Mycopathologia* **2008**, *166*, 93–102. [[CrossRef](#)] [[PubMed](#)]
55. Chen, X.; Zhao, X.; Deng, Y.; Bu, X.; Ye, H.; Guo, N. Antimicrobial potential of myristic acid against *Listeria monocytogenes* in milk. *J. Antibiot.* **2019**, *72*, 298–305. [[CrossRef](#)] [[PubMed](#)]
56. Prasath, K.G.; Sethupathy, S.; Pandian, S.K. Proteomic analysis uncovers the modulation of ergosterol, sphingolipid and oxidative stress pathway by myristic acid impeding biofilm and virulence in *Candida albicans*. *J. Proteom.* **2019**, *208*, 103503. [[CrossRef](#)] [[PubMed](#)]
57. Carballeira, N.M.; O'Neill, R.; Parang, K. Synthesis and antifungal properties of  $\alpha$ -methoxy and  $\alpha$ -hydroxyl substituted 4-thiatetradecanoic acids. *Chem. Phys. Lipids* **2007**, *150*, 82–88. [[CrossRef](#)]
58. Lee, J.-Y.; Kim, Y.-S.; Shin, D.-H. Antimicrobial Synergistic Effect of Linolenic Acid and Monoglyceride against *Bacillus cereus* and *Staphylococcus aureus*. *J. Agric. Food Chem.* **2002**, *50*, 2193–2199. [[CrossRef](#)]
59. Raynor, L.; Mitchell, A.; Walker, R. Antifungal Activities of Four Fatty Acids against Plant Pathogenic Fungi. *Mycopathologia* **2004**, *157*, 87–90. [[CrossRef](#)] [[PubMed](#)]
60. Al-Salih, D.A.A.K.; Aziz, F.M.; Mshimesh, B.A.R.; Jihad, M.T. Antibacterial effects of vitamin E: In vitro study. *J. Biotechnol. Res. Cent.* **2013**, *7*, 17–23.
61. Baran, R.; Thomas, L. Combination of fluconazole and alpha-tocopherol in the treatment of yellow nail syndrome. *J. Drugs Dermatol. JDD* **2009**, *8*, 276–278.
62. Yeamsuksawat, T.; Liang, J. Characterization and release kinetic of crosslinked chitosan film incorporated with  $\alpha$ -tocopherol. *Food Packag. Shelf Life* **2019**, *22*, 100415. [[CrossRef](#)]

63. Martins, J.T.; Cerqueira, M.; Vicente, A.A. Influence of  $\alpha$ -tocopherol on physicochemical properties of chitosan-based films. *Food Hydrocoll.* **2012**, *27*, 220–227. [[CrossRef](#)]
64. Raza, Z.A.; Abid, S.; Azam, A.; Rehman, A. Synthesis of alpha-tocopherol encapsulated chitosan nano-assemblies and their impregnation on cellulosic fabric for potential antibacterial and antioxidant cosmetotextiles. *Cellulose* **2019**, *27*, 1717–1731. [[CrossRef](#)]
65. Liu, C.-G.; Desai, K.G.H.; Chen, A.X.-G.; Park, H.-J. Linolenic Acid-Modified Chitosan for Formation of Self-Assembled Nanoparticles. *J. Agric. Food Chem.* **2004**, *53*, 437–441. [[CrossRef](#)] [[PubMed](#)]
66. Kurniasih, M.; Purwati; Dewi, R.S. Toxicity tests, antioxidant activity, and antimicrobial activity of chitosan. *IOP Conf. Ser. Mater. Sci. Eng.* **2018**, *349*, 012037. [[CrossRef](#)]
67. Rajaei, A.; Hadian, M.; Mohsenifar, A.; Rahmani-Cherati, T.; Tabatabaei, M. A coating based on clove essential oils encapsulated by chitosan-myristic acid nanogel efficiently enhanced the shelf-life of beef cutlets. *Food Packag. Shelf Life* **2017**, *14*, 137–145. [[CrossRef](#)]
68. Langa-Lomba, N.; Buzón-Durán, L.; Martín-Ramos, P.; Casanova-Gascón, J.; Martín-Gil, J.; Sánchez-Hernández, E.; González-García, V. Assessment of Conjugate Complexes of Chitosan and *Urtica dioica* or *Equisetum arvense* Extracts for the Control of Grapevine Trunk Pathogens. *Agronomy* **2021**, *11*, 976. [[CrossRef](#)]
69. Sánchez-Hernández, E.; Buzón-Durán, L.; Andrés-Juan, C.; Lorenzo-Vidal, B.; Martín-Gil, J.; Martín-Ramos, P. Physicochemical Characterization of *Crithmum maritimum* L. and *Daucus carota* subsp. *gummifer* (Syme) Hook.fil. and Their Antimicrobial Activity against Apple Tree and Grapevine Phytopathogens. *Agronomy* **2021**, *11*, 886. [[CrossRef](#)]
70. Liang, C.; Yuan, F.; Liu, F.; Wang, Y.; Gao, Y. Structure and antimicrobial mechanism of  $\epsilon$ -polylysine–chitosan conjugates through Maillard reaction. *Int. J. Biol. Macromol.* **2014**, *70*, 427–434. [[CrossRef](#)] [[PubMed](#)]
71. Buzón-Durán, L.; Langa-Lomba, N.; González-García, V.; Casanova-Gascón, J.; Martín-Gil, J.; Pérez-Lebeña, E.; Martín-Ramos, P. On the Applicability of Chitosan Oligomers-Amino Acid Conjugate Complexes as Eco-Friendly Fungicides against Grapevine Trunk Pathogens. *Agronomy* **2021**, *11*, 324. [[CrossRef](#)]
72. Buzón-Durán, L.; Martín-Gil, J.; Marcos-Robles, J.L.; Fombellida-Villafruela, A.; Pérez-Lebeña, E.; Martín-Ramos, P. Antifungal Activity of Chitosan Oligomers–Amino Acid Conjugate Complexes against *Fusarium culmorum* in Spelt (*Triticum spelta* L.). *Agronomy* **2020**, *10*, 1427. [[CrossRef](#)]
73. Buzón-Durán, L.; Martín-Gil, J.; Pérez-Lebeña, E.; Ruano-Rosa, D.; Revuelta, J.L.; Casanova-Gascón, J.; Ramos-Sánchez, M.C.; Martín-Ramos, P. Antifungal Agents Based on Chitosan Oligomers,  $\epsilon$ -polylysine and *Streptomyces* spp. Secondary Metabolites against Three Botryosphaeriaceae Species. *Antibiotics* **2019**, *8*, 99. [[CrossRef](#)] [[PubMed](#)]
74. Santos-Moriano, P.; Fernandez-Arrojo, L.; Mengíbar, M.; Belmonte-Reche, E.; Peñalver, P.; Acosta, F.N.; Ballesteros, A.O.; Morales, J.C.; Kidibule, P.; Fernandez-Lobato, M.; et al. Enzymatic production of fully deacetylated chitoooligosaccharides and their neuroprotective and anti-inflammatory properties. *Biocatal. Biotransform.* **2017**, *36*, 57–67. [[CrossRef](#)]
75. Martin, M.T.; Cobos, R. Identification of Fungi Associated with Grapevine Decline in Castilla y León (Spain). *Phytopathol. Mediterr.* **2007**, *46*, 18–25. [[CrossRef](#)]
76. Talwalkar, A.T. *IGT/DOE Coal-Conversion Systems Technical Data Book*; Institute of Gas Technology: Chicago, IL, USA, 1981; p. 23.
77. Jallali, I.; Zaouali, Y.; Missaoui, I.; Smeoui, A.; Abdelly, C.; Ksouri, R. Variability of antioxidant and antibacterial effects of essential oils and acetonic extracts of two edible halophytes: *Crithmum Maritimum* L. and *Inula Crithmoides* L. *Food Chem.* **2014**, *145*, 1031–1038. [[CrossRef](#)] [[PubMed](#)]
78. Langa-Lomba, N.; Sánchez-Hernández, E.; Buzón-Durán, L.; González-García, V.; Casanova-Gascón, J.; Martín-Gil, J.; Martín-Ramos, P. Activity of Anthracenediones and Flavoring Phenols in Hydromethanolic Extracts of *Rubia tinctorum* against Grapevine Phytopathogenic Fungi. *Plants* **2021**, *10*, 1527. [[CrossRef](#)]
79. CLSI. *Methods for Dilution Antimicrobial Susceptibility Tests for Bacteria that Grow Aerobically*, 11th ed.; CLSI standard M07; Clinical and Laboratory Standards Institute: Wayne, PA, USA, 2018.
80. Arendrup, M.C.; Cuenca-Estrella, M.; Lass-Flörl, C.; Hope, W. EUCAST technical note on the EUCAST definitive document EDef 7.2: Method for the determination of broth dilution minimum inhibitory concentrations of antifungal agents for yeasts EDef 7.2 (EUCAST-AFST). *Clin. Microbiol. Infect.* **2012**, *18*, E246–E247. [[CrossRef](#)]
81. Levy, Y.; Benderly, M.; Cohen, Y.; Gisi, U.; Bassand, D. The joint action of fungicides in mixtures: Comparison of two methods for synergy calculation. *EPP0 Bull.* **1986**, *16*, 651–657. [[CrossRef](#)]